AIP Advances

A position control method for a robotically assisted magnetic navigation system to improve the pushability of a magnetic catheter by maximizing magnetic force

Cite as: AIP Advances **13**, 035119 (2023); https://doi.org/10.1063/9.0000390
Submitted: 28 September 2022 • Accepted: 10 February 2023 • Published Online: 12 March 2023

D. Lee, E. Jung, J. Kwon, et al.

A position control method for a robotically assisted magnetic navigation system to improve the pushability of a magnetic catheter by maximizing magnetic force

Cite as: AIP Advances 13, 035119 (2023); doi: 10.1063/9.0000390
Submitted: 28 September 2022 • Accepted: 10 February 2023 •
Published Online: 13 March 2023

D. Lee, E. Jung, J. Kwon, and G. Jang[a)]

AFFILIATIONS

PREM, Department of Mechanical Engineering, Hanyang University, Seoul 04763, South Korea

Note: This paper was presented at the 67th Annual Conference on Magnetism and Magnetic Materials.
[a)]**Author to whom correspondence should be addressed:** ghjang@hanyang.ac.kr

ABSTRACT

We propose a novel position control method (PCM) for the Robotically Assisted MAgnetic Navigation (RAMAN) system to improve the pushability of the magnetic catheter (MC) by maximizing the magnetic force. We expressed the magnetic force acting on the magnetic catheter as the position and the current flowing through each of the electromagnets of the RAMAN system. Next, we formulated a PCM as an optimization problem to maximize the MF. From the proposed PCM, we can determine the position that generates the maximum MF in the desired direction within the region of interest of the RAMAN as well as the required applied current of each electromagnet. Finally, we performed a navigation experiment for the MC along the aorta to the right coronary artery in a cardiac vascular phantom model, and we showed that the proposed PCM can navigate through the vascular phantom effectively without buckling of the MC.

I. INTRODUCTION

Occlusive vascular disease is one of the major causes of death in modern society, and endovascular intervention, a minimally invasive medical procedure, has been developed to treat such diseases. In endovascular intervention, medical doctors utilize a guide wire or a catheter along the blood vessel to reach a target lesion and perform medical treatment. However, it is not easy for a medical doctor to steer the direction of the distal end of the catheter in the blood vessel accurately by manually controlling the proximal end of the catheter in the outside of the patient's body.[1,2] To overcome this limitation, a magnetic catheter (MC) controlled by a magnetic navigation system (MNS) and a feeding device have been developed to improve the steerability of conventional catheters.[3,4] An external magnetic field (EMF) generated from the MNS generates magnetic torque at the permanent magnets (PMs) in the MC to remotely steer the MC's distal end, while the feeding device pushes the proximal end of the MC to move the MC forward.[3,4] However, the feeding device also pushes the proximal end of the catheter, and sometimes the feeding force is not efficiently transmitted to the distal end of the MC. In this case, the MC does not move in the axial direction and the flexible part of the MC bends due to the buckling effect, resulting in a loss of pushability. As shown in Fig. 1(a), blood vessels such as the aorta have a large inner diameter compared to the diameter of an MC and have a complex shape. To push the MC in these blood vessels in the right direction, it is essential to generate a force that pulls the distal end to avoid buckling. A magnetic force (MF) generated by the MNS is a possible candidate for the pulling forces.

We propose a position control method (PCM) for the Robotically Assisted MAgnetic Navigation (RAMAN) system to improve the pushability of the MC by maximizing the MF. Fig. 1(b) shows the developed RAMAN system in which a 7-axis stage robot can move the 8 electromagnets in order to move the region of interest (ROI) surrounded by them. We expressed the MF acting on the MC as the position and the current flowing through each of the 8 electromagnets. Next, we formulated the PCM as an optimization problem

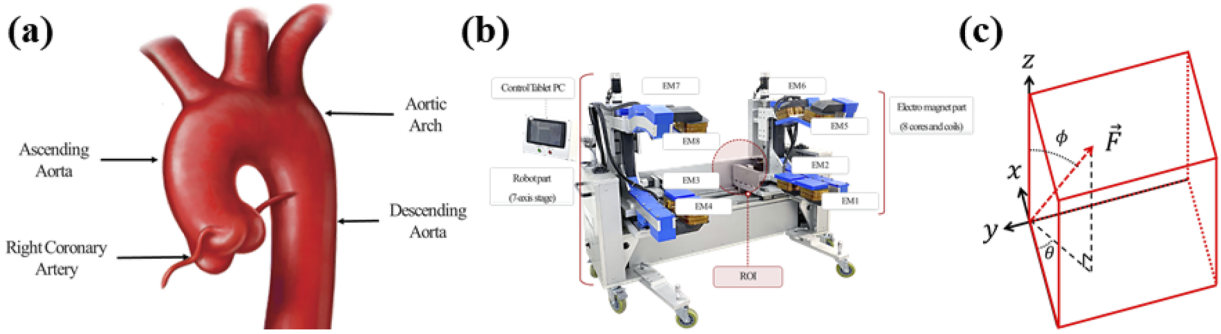

FIG. 1. (a) Aorta with a diameter of 2–3 cm, (b) RAMAN and ROI, (c) Coordinate axes in ROI and direction of MF.

to maximize the MF. From the proposed PCM, we can determine the position that generates the maximum MF in the desired direction within the ROI of the RAMAN as well as the required applied current of each electromagnet. Finally, we performed a navigation experiment for the MC along the aorta to the right coronary artery in a cardiac vascular phantom model, and we showed that the proposed PCM can release the buckled catheter effectively.

II. PCM OF THE RAMAN SYSTEM

The developed RAMAN system consists of a robot and electromagnet parts. The robot has a total of 7 degrees of freedom. The four left and right electromagnets each have translational motion along the x and y axes, while the four upper and lower electromagnets each have translational motion along the z-axis, and all of eight electromagnets together have translational motion along the z-axis. In the electromagnet part, the tips of the eight electromagnets are composed of eight vertices of a cuboid. The width (x-axis), length (y-axis), and height (z-axis) of this cuboid are 212, 317, and 350 mm, respectively. We set 80% of the space to the ROI of the RAMAN system, excluding the height of the patient bed (50 mm), the safety distance between the patient bed and the lower electromagnet (10 mm), and the safety distance between the patient and the upper electromagnet (10 mm).

A magnetic field can be generated by applying an electric current to the electromagnets of the RAMAN system. When the magnetic field is in a linear relationship with the applied current of the electromagnets of the RAMAN system, the magnetic flux density generated by each electromagnet at an arbitrary position in the ROI can be superposed with the magnetic flux density generated by each electromagnet as follows:

$$\boldsymbol{B} = \{\boldsymbol{A_B}(\boldsymbol{P})\} \cdot \boldsymbol{I} \tag{1}$$

where $\boldsymbol{B}$, $\boldsymbol{P}$, $\{\boldsymbol{A_B}(\boldsymbol{P})\}$, $\boldsymbol{I} = [I_1 \ldots I_8]^T$ is the vector of the magnetic flux density, position vector, actuation matrix, and applied currents to eight electromagnet, respectively. The i-th row and j-th column of the actuation matrix is the generated magnetic flux density along the i-th direction when a unit current is applied to the j-th electromagnet. To determine the field actuation matrix, we divided the ROI into 11 points in the x, y, and z directions, and applied a unit current to each electromagnet. Then, we measured the magnetic flux density along the x, y, and z directions. We performed this measurement for the 1,331 points (11 × 11 × 11) in the ROI.

The magnetic torque and force acting on the PM of the MC by the external magnetic flux density can be respectively expressed as Eqs. (2) and (3) as follows:

$$\boldsymbol{T} = \boldsymbol{m} \times \boldsymbol{B} \tag{2}$$

$$\boldsymbol{F} = (\boldsymbol{m} \cdot \nabla)\boldsymbol{B} \tag{3}$$

where $\boldsymbol{m}$ is the magnetic dipole moment of the PM. From Eqs. (1) and (3), we can rewrite the magnetic force as follows:

$$\boldsymbol{F} = (\boldsymbol{m} \cdot \nabla)\{\boldsymbol{A_B}(\boldsymbol{P})\} \cdot \boldsymbol{I} \tag{4}$$

Once we expand the actuation matrix of the magnetic force by including $\boldsymbol{A_F}(\boldsymbol{m}, \boldsymbol{P}) = (\boldsymbol{m} \cdot \nabla)\{\boldsymbol{A_B}(\boldsymbol{P})\}$, the magnetic flux density and the magnetic force at a position $\boldsymbol{P}$ in the ROI can be written as follows:

$$\begin{bmatrix} \boldsymbol{B} \\ \boldsymbol{F} \end{bmatrix} = \begin{Bmatrix} \boldsymbol{A_B}(\boldsymbol{P}) \\ \boldsymbol{A_F}(\mathbf{m}, \boldsymbol{P}) \end{Bmatrix} \cdot \boldsymbol{I} \tag{5}$$

The PM attached to the distal end of the MC is axially magnetized. The magnetic torque aligns the magnetization direction of the PM along the same direction as the EMF, and we need the magnetic force acting on the PM along the same direction as the EMF to pull the MC. Therefore, the directions of the EMF and MF generated by the RAMAN system are the same as shown in Fig. 1(c). When the direction of the magnetization direction is (θ, φ), a unit directional vector $\boldsymbol{e_{dir}}$ of the EMF and the magnetic force can be expressed as follows:

$$[\boldsymbol{e_{dir}}] = \begin{bmatrix} \cos\theta \cdot \sin\varphi \\ \sin\theta \cdot \sin\varphi \\ \cos\varphi \end{bmatrix} \tag{6}$$

We formulated the optimization problem to maximize the magnetic force acting on the MC along the $\boldsymbol{e_{dir}}$ at a position $\boldsymbol{P}$ inside the ROI of the RAMAN system as shown in the following Eq. (7).

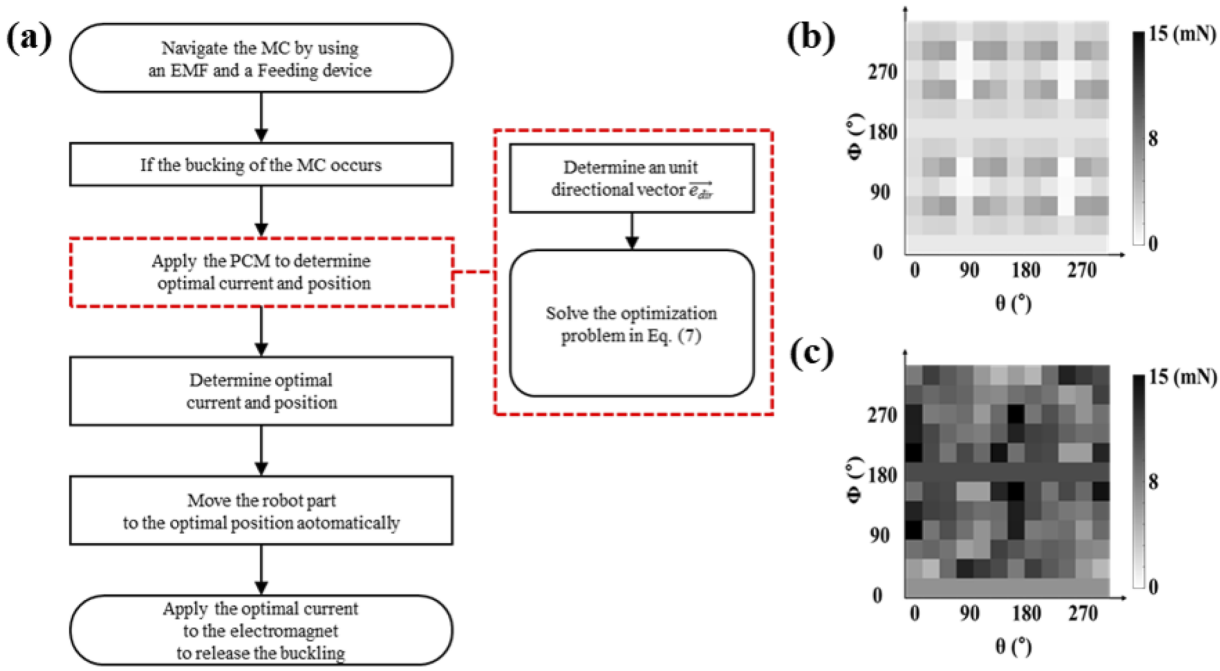

FIG. 2. (a) The PCM control method used to determine the maximum magnetic force, (b) the maximum magnetic force at the center of the ROI, (c) the maximum magnetic force at the proposed position according to the change of θ and φ directions.

$$\begin{aligned} &\textbf{Maximize } F(I,P) = \|\{A_F(\mathbf{m},P)\}\cdot I\| \\ &\textbf{subject to } \{A_B(P)\}\cdot I \,//\, e_{dir},\ \{A_F(m,P)\}\cdot I \,//\, e_{dir}, \\ &\text{and } I_n \le 15\ (n=1,\ldots,8) \end{aligned} \tag{7}$$

The above optimization problem determines the current of each electromagnet to generate the maximized magnetic force along the e_{dir} direction at the arbitrary position P. To determine the optimal position P to maximize magnetic force in the whole ROI, we used the fact that the magnitude of the magnetic force acting on the PM increases as it approaches the electromagnet. To maximize the magnetic force along the desired direction e_{dir} inside the ROI, we solved the optimization problem from Eq. (7) for each of the eight vertices of the electromagnet of the RAMAN system. After solving each of the eight optimization problems, the position to generate the largest magnetic force is determined as the optimal position. Fig. 2(a) shows the flow chart of the proposed PCM to determine the optimal position to generate the maximum magnetic force.

III. RESULTS AND DISCUSSION

First, we performed a simulation of the proposed PCM within the ROI of the developed RAMAN system. To confirm that the proposed PCM can effectively generate the magnetic force in all directions, we divided the direction of the magnetic force by 30-degree intervals along the θ and φ directions and calculated the magnetic force in each direction. As shown in Figs. 2(b) and 2(c), the proposed method can generate a large magnetic force compared to the case without the application of the PCM. Without the application of the PCM, the magnetic force has a minimum of 0.12 mN, a maximum of 5.71 mN, and an average of 2.54 mN at the origin of the ROI of the RAMAN system depending on the direction of the magnetic force. However, with the application of the PCM, we can generate the magnetic force with a minimum of 4.18 mN, a maximum of 16.81 mN, and an average of 9.15 mN at the optimal position depending on the direction of the magnetic force. It shows that the PCM can generate an average magnetic force 3.5 times larger than the case without PCM.

Finally, we performed an experiment to determine whether the PCM can overcome the buckling of the MC within blood vessel. We prototyped the MC with a PM attached to its distal part. The prototyped MC had an axially magnetized PM of NdFeB 52 (m = 1.45 A m^2) with an outer diameter of 2 mm, an inner diameter of 1 mm, and a length of 10 mm at the distal part. As shown in Fig. 3(a), we performed a navigation experiment for the MC in an aortic vascular phantom model, which enters the descending aorta, passes the aortic arch and the ascending aorta, and then enters the right coronary artery of the heart. Without the application of the PCM, buckling of the MC occurred as it passed through the aortic arch as shown in Fig. 3(b). In this position, the RAMAN system can generate the magnetic force of 2.56 mN but it is not sufficient to overcome the buckling of the MC. However, with the application of the PCM, the RAMAN system can generate the magnetic force of 8.68 mN and it is sufficient to overcome the buckling of the MC as shown in Fig. 3(c).

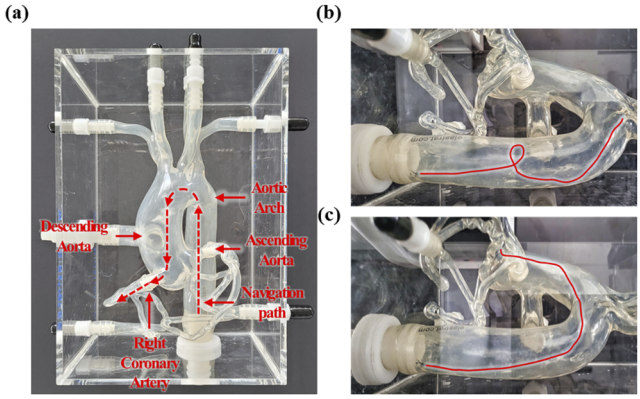

FIG. 3. (a) Aortic vascular phantom model and navigation path, (b) buckling of the MC, (c) successful navigation of the MC with the application of the PCM (we overlay the MC along the aorta).

We can successfully steer and pull the MC to the right coronary artery by utilizing the proposed PCM.

IV. CONCLUSION

We proposed a PCM to maximize the magnetic force generated by the RAMAN system to improve the pushability of the MC. We show that the proposed PCM can generate an average magnetic force 3.5 times larger than the case without the application of the PCM. Next, we performed an experiment to show that the proposed PCM can overcome the buckling of an MC when the MC navigates along the blood vessel. Without the application of the PCM, we observed the buckling of MC in the aortic vascular phantom, and we cannot further steer the MC. With the application of the PCM, we can overcome the buckling of the MC and we successfully steer and pull the MC to the right coronary artery. This research will contribute to treating occlusive vascular disease by improving the pushability of the MC.

ACKNOWLEDGMENTS

This research was supported by a grant of the Korea Health Technology R & D Project through the Korea Health Industry Development Institute (KHIDI), funded by the Ministry of Health & Welfare, Republic of Korea (Grant Number: HI19C1055).

AUTHOR DECLARATIONS

Conflict of Interest

The authors have no conflicts to disclose.

Author Contributions

D. Lee: Conceptualization (lead); Investigation (lead); Software (lead); Writing – original draft (lead). **E. Jung**: Software (supporting); Writing – original draft (supporting). **J. Kwon**: Investigation (supporting); Writing – original draft (supporting). **G. Jang**: Funding acquisition (lead); Project administration (lead); Supervision (lead); Writing – review & editing (lead).

DATA AVAILABILITY

The data that support the findings of this study are available from the corresponding author upon reasonable request.

REFERENCES

[1] B. J. Nelson, I. K. Kaliakatsos, and J. J. Abbott, Annu. Rev. Biomed. Eng. **12**, 55 (2010).
[2] N. Kim, S. Lee, W. Lee, and G. Jang, AIP Advances **8**, 056708 (2018).
[3] J. Nam, W. Lee, E. Jung, and G. Jang, IEEE Transactions on Industrial Electronics **65**, 5673 (2018).
[4] E. Jung, W. Lee, N. Kim, J. Kim, J. Park, and G. Jang, AIP Advances **9**, 125230 (2019).